

Conservation of complex knotting and slipknotting patterns in proteins

Joanna I. Sułkowska^{a,1,2}, Eric J. Rawdon^{b,1}, Kenneth C. Millett^c, Jose N. Onuchic^{d,2}, and Andrzej Stasiak^e

^aCenter for Theoretical Biological Physics, University of California at San Diego, La Jolla, CA 92037; ^bDepartment of Mathematics, University of St. Thomas, Saint Paul, MN 55105; ^cDepartment of Mathematics, University of California, Santa Barbara, CA 93106; ^dCenter for Theoretical Biological Physics, Rice University, Houston, TX 77005; and ^eCenter for Integrative Genomics, Faculty of Biology and Medicine, University of Lausanne, 1015 Lausanne, Switzerland

Edited by* Michael S. Waterman, University of Southern California, Los Angeles, CA, and approved May 4, 2012 (received for review April 17, 2012)

While analyzing all available protein structures for the presence of knots and slipknots, we detected a strict conservation of complex knotting patterns within and between several protein families despite their large sequence divergence. Because protein folding pathways leading to knotted native protein structures are slower and less efficient than those leading to unknotted proteins with similar size and sequence, the strict conservation of the knotting patterns indicates an important physiological role of knots and slipknots in these proteins. Although little is known about the functional role of knots, recent studies have demonstrated a protein-stabilizing ability of knots and slipknots. Some of the conserved knotting patterns occur in proteins forming transmembrane channels where the slipknot loop seems to strap together the transmembrane helices forming the channel.

protein knots | knot theory | topology

There are increasing numbers of known proteins that form linear open knots in their native folded structure (1, 2). In general, knots in proteins are orders of magnitude less frequent than would be expected for random polymers with similar length, compactness, and flexibility (3). In principle, the polypeptide chains folding into knotted native protein structures encounter more kinetic difficulties than unknotted proteins (4–12). Therefore, it is believed that knotted protein structures were, in part, eliminated during evolution because proteins that fold slowly and/or nonreproducibly should be evolutionarily disadvantageous for the hosting organisms. Nevertheless, there are several families of proteins that reproducibly form simple knots, complex knots, and slipknots (1, 2). In these proteins, the disadvantage of less efficient folding may be balanced by a functional advantage connected with the presence of these knots. Numerous experimental (13–16) and theoretical (17–27) studies have been devoted to understanding the precise nature of the structural and functional advantages created by the presence of these knots in protein backbones. It has been proposed that in some cases the protein knots and slipknots provide a stabilizing function that can act by holding together certain protein domains (4). In the majority of cases, however, one is unable to determine the precise structural and functional advantages provided by the presence of knots.

To shed light on the function and formation of protein knots, we performed a thorough characterization of knotting within protein structures deposited in the Protein Data Bank (PDB) (28) by creating a precise mapping of the position and size of the knotted and slipknotted domains and knot tails (1, 2). We identified the types of knots that are formed by the backbone of the entire polypeptide chain and also by all continuous backbone portions of a given protein (1, 2). To characterize the knotting of proteins with linear backbones, one needs to set aside the orthodox rule of knot theory that states that all linear chains are unknotted because, by a continuous deformation, one can always disentangle even highly entangled linear chain into one that follows a straight line. Of course, the characterization of the knotting within the protein structures makes sense only if one consid-

ers fixed configurations, in this case proteins in their native folded structures. Then they may be treated as frozen and thus unable to undergo any deformation.

Several papers have described various interesting closure procedures to capture the knot type of the native structure of a protein or a subchain of a closed chain (1, 3, 29–33). In general, the strategy is to ensure that the closure procedure does not affect the inherent entanglement in the analyzed protein chain or subchain. Unfortunately, this approach works well only for some of the possible linear configurations. In other cases, the resulting knot type is not uniquely determined by the geometry of the linear fragment but is strongly affected by parameters of the specific closure algorithm. Another strategy for characterizing the knotting of linear fragments is to keep the ends of the linear fragment fixed in space and to “simplify” the chain by a triangle elimination method or some other chain shortening procedure that avoids intersegmental passages (29, 34). When the shortening procedure has exhausted all simplifications on a protein configuration, one usually obtains configurations with the ends protruding from the entangled portion. It is then easy to connect the ends without passing through the entangled portion. However, the shortening method applied to the same starting configuration can result in different knot types depending on the order of the shortening moves (30). Because the order of the shortening moves is not determined by the actual configuration but depends on arbitrarily chosen parameters, this method also is confronted with the problem that the linear chains do not totally determine the knot type of the frozen chain.

Limitations in these single closure methods stimulated interest in probabilistic methods of defining the most likely knot type of linear chains with a given geometry (1, 3, 30). One relatively simple, unbiased method consists of placing the analyzed linear chain near the center of a large sphere and closing it by adding to each end one long segment connecting it with the same, randomly chosen point on the enclosing sphere. When this procedure is repeated many times, one obtains a spectrum of knots determined by the given linear fragment (30). Knot types that are dominant (i.e., the knot type occurring most frequently) in the resulting spectrum can be considered as characterizing the knotting of the linear fragment (1, 3, 30). In our characterization of the knotting with the protein structures, we apply a uniform closure procedure inspired by Millett et al. (30).

Author contributions: J.I.S., E.J.R., K.C.M., J.N.O., and A.S. designed research; J.I.S. and E.J.R. performed research; E.J.R. and K.C.M. contributed new reagents/analytic tools; J.I.S., E.J.R., K.C.M., J.N.O., and A.S. analyzed data; and J.I.S., E.J.R., K.C.M., J.N.O., and A.S. wrote the paper.

The authors declare no conflict of interest.

*This Direct Submission article had a prearranged editor.

¹J.I.S. and E.J.R. contributed equally to this work.

²To whom correspondence may be addressed. E-mail: jonuchic@rice.edu or jsulkow@physics.ucsd.edu.

This article contains supporting information online at www.pnas.org/lookup/suppl/doi:10.1073/pnas.1205918109/-DCSupplemental.

In addition to analyzing the complete polypeptide chains, we also analyzed all continuous subchains to detect knots and slipknots (2). By identifying the knot type of each subchain, we are able to locate the cores of the knots—i.e., the minimal portions of the protein backbones that form a given knot type.

Classification of Knotting in Protein Structures

We analyzed 74,223 structures submitted to the PDB through April 2011 and determined their global and local knotting. In this large set of structures, we found 398 knotted and 222 slipknotted proteins including 64 different carbonic anhydrases sequences. We divided all proteins with knots and slipknots according to the complexity of their knotting. Table 1 lists representative protein family members with complex knotting, whereas the tables in the *SI Appendix* (see *SI Appendix*, Tables S1 and S2) list those with simple knotting.

The paths of native polypeptide chains are complex. Even using modern computer graphics of protein structures, it is difficult to detect whether a given protein forms a knot and where the knot is located simply by looking at the structure. For this reason, it has been useful to develop ways to visualize the knotting landscape of protein structures in the form of a matrix (2, 36) in which every entry represents the knot type of a different subchain of the native polypeptide chain.

Each entry in the matrix indicates knotting in the subchain starting with the amino acid position indicated on the horizontal axis and ending with the amino acid position indicated on the vertical axis (see Fig. 1). Therefore, the entry in the lower left corner reports the knotting of the entire polypeptide chain in its folded configuration. Entries approaching the diagonal correspond to shorter and shorter subchains.

The identity and strength of the knotting character of each subchain is reported by employing distinct shaded color schemes for each knot type in Figs. 2–5. The schematic presentation in Fig. 1*A* illustrates the case in which the entire protein forms a 3_1 knot. In such a case, entries at or close to the lower left-hand corner show that the entire protein and subchains encompassing nearly the entire protein form a 3_1 knot. Moving up and/or to the right within the matrix, we eventually reach entries that indicate the unknotted character of the corresponding subchains. If the removal of only a few amino acids from the N or C terminus is sufficient to unknot the fragment, the knot is considered shallow. The entry closest to the diagonal of the matrix that indicates a knotted state in the corresponding subchain gives the size of

the knotted core—i.e., the shortest portion of the chain that still forms the given knot type.

Another situation is shown in Fig. 1*B* and *C*, which represent slipknot configurations. In those cases, the entire protein is unknotted but it contains at least one subchain forming a nontrivial knot (for example, this is the case of a shoelace bow). Slipknots in unknotted proteins can be recognized when the entries at or near the lower left-hand corner report an unknotted state but, as one or both ends are trimmed (moving up and/or to the right in the matrix), a knotted subchain is formed.

Table 1 lists the observed knotted and slipknotted proteins in decreasing order of their knotting complexity. In their knotting notation, we list all dominant knot types formed by their various subchains, ordered by length from longest to shortest. For example, the notation $K6_1, 4_1, 3_1$ indicates that the various subchains form 6_1 , 4_1 , and 3_1 knots. The letter K indicates that the entire protein is knotted. The double presence of the 6_1 knot means that, in the matrix representation of the protein knotting, there are two disjoint “territories” that form a 6_1 knot (see Fig. 2). The notation $S3_1, 3_1, 3_1$ indicates that the entire protein chain forms a slipknot (denoted by S) with four disjoint 3_1 territories in the matrix presentation of the protein (see Fig. 5). Table 1 also shows the names of the protein families to which a given knotted protein belongs, the corresponding PDB access codes, and whether the knotted character of a given protein was established in this study. In several cases, listed in the table and indicated with ^a and ^b, the structure determination was not complete, resulting in an uncertainty concerning the position of some fragments. For our analysis, we replaced missing fragments with a straight line if the missing peptide could be placed in the vicinity of the straight line without clashing with the rest of the chain, indicated by ^a. In one case (1cmx), indicated by ^b, the missing peptide had to follow an arc to avoid a steric clash with the rest of the determined protein structure. The path of this arc was chosen based on the structure of homologous proteins with better resolved crystals.

Knotting Fingerprints of Proteins with Complex Knot Types

Stevedore’s Protein Knot. The most complex protein knot currently known is formed by the backbone of α -haloacid dehalogenase DehI (27). DehI is a bacterial enzyme hydrolyzing carbon–halogen bonds and is therefore capable of biodegrading environmental pollutants such as herbicides and pesticides (37). The crystal structure of DehI has been known since 2008 (37) but it was only in 2010 that its Stevedore’s knot (6_1 in knot tables) structure was

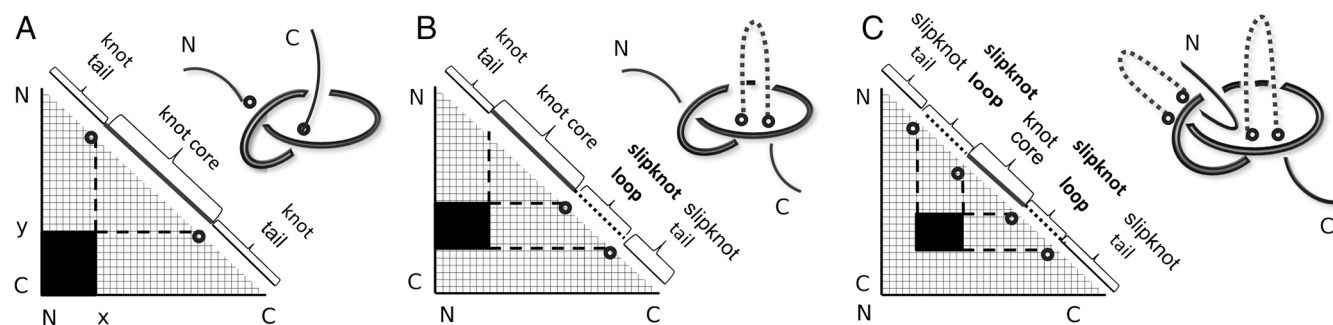


Fig. 1. Matrix presentations of protein knotting. Each entry in the matrix indicates the knot type formed by one continuous subchain by its shading (Fig. 1) or color (Figs. 2–5). In each case, the subchain starts with the N-terminal amino acid at position x and ends with the C-terminal amino acid at position y , indicated on the horizontal and vertical axes, respectively. Equivalently, this subchain can be interpreted as a part of the diagonal, delimited by the corresponding coordinates x and y , where the entire diagonal corresponds to the entire polypeptide chain. (A) A case of a knotted protein. Notice that the entry in the lower left-hand corner, which corresponds to the entire protein, is shaded; this indicates that the corresponding chain or subchain is knotted. The knot core is defined as the shortest subchain that still forms a knot (see the thickened part of the protein in the sketch above). The two remaining parts of the chain form knot tails, and their length is conveniently represented along the diagonal. Subchains that do not include at least short bits of both knot tails do not form knots and therefore the matrix entries corresponding to these subchains are not shaded. (B and C) Cases of protein slipknots. Notice that in the case of slipknots the entire protein is unknotted (the element in the lower corner is white) but as one (B) or both termini (C) are trimmed to some extent, the remaining fragment forms a trefoil knot, denoted 3_1 in Table 1 and *SI Appendix*, Table S2, and the corresponding matrix entries are therefore darkened in the matrix. Schematic drawings of the polypeptide chains forming trefoil knots and slipknots illustrate which parts of the polypeptide chains constitute the knot cores (thickened), the knot and slipknot tails (solid line), and the slipknot loops (dashed line).

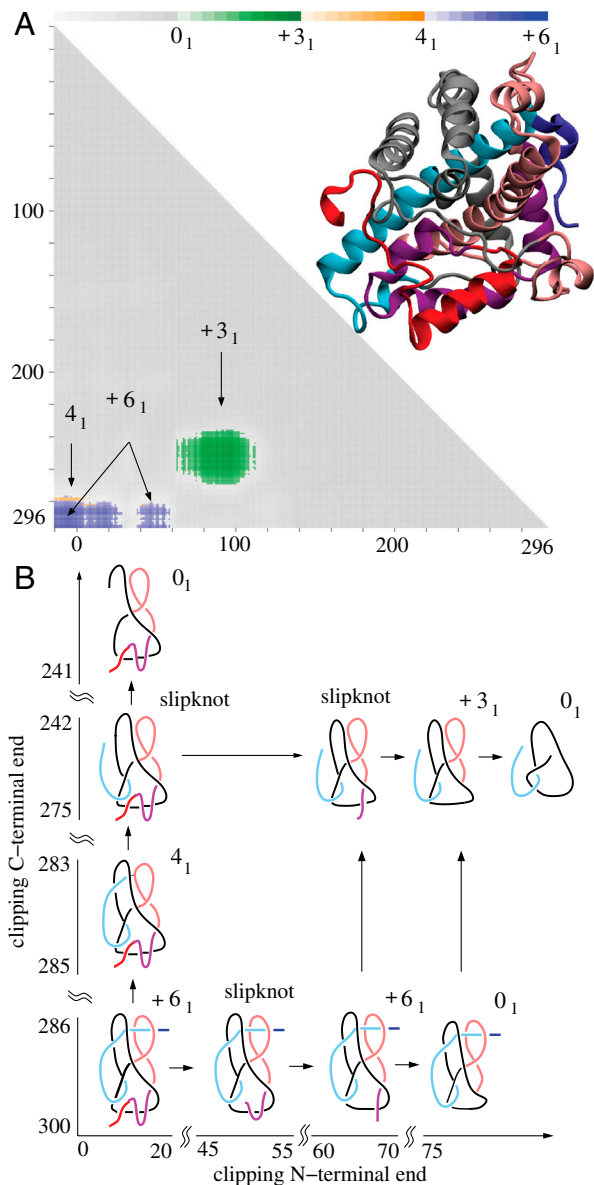


Fig. 2. The Dehl protein forms the Stevedore's knot as a whole but some of its subchains form 4_1 and 3_1 knots or form Stevedore's and trefoil slipknots. (A) Matrix presentation of the Dehl knotting. The color scale shows the dominant knot type formed by a given subchain and the frequency (shown via the color opacity) of its formation. The color bar above a matrix presents the corresponding frequencies at 10%, 20%, ..., 100%. Notice the narrow territory of 4_1 knots above the territory of the Stevedore's knot. (B) Schematic drawing explaining how the progressive clipping of the C and/or N terminus from the entire polypeptide chain with Stevedore's knot leads to subchains forming 4_1 and 3_1 knots or Stevedore's and trefoil slipknots.

recognized (27). Fig. 2 shows the results of the knotting analysis of all linear subchains within the crystal structure of DehI. The elementary square in the lower left-hand corner with coordinates (1,310), shows that the entire protein forms the 6_1 knot. However, when smaller subchains are considered, these form 4_1 (figure-eight) and 3_1 knots. It may seem surprising that subchains of a protein, which as a whole forms the 6_1 knot, can result in the formation of other nontrivial knot types.

Therefore, let us explain how this knotting pattern occurs. Fig. 2B shows, in schematic form, the essential geometric features of the entire DehI protein backbone and its relevant subchains. Drawings representing the protein subchains resulting from progressively clipping the C terminus are placed above the entire

Table 1. Complex knotting patterns in proteins and their conservation

Motif	Family	Protein/PDB	Source
$K_{6_1 6_1 4_1 3_1}$	α -haloacid dehalogenase	DehI/3bjx	<i>Arthrobacter siderocaspulatus</i>
$K_{5_2 3_1 3_1}$	ubiquitin C-terminal hydrolase	UCHL1/3irt UCHL3/1xd3 UCHL3/2wdt [n] UCHL5/3a7s ^a [n] Yuh1/1cmx ^b	Human Human <i>P. falciparum</i> Human Yeast
$S_{3_1 4_1 3_1}$	SNF	LeuT(Aa)/2a65	<i>Aquifex aeolicus</i>
$S_{3_1 4_1 3_1}$	NCS1	Mhp1/2jlo [n]	<i>M. liquefaciens</i>
$S_{3_1 4_1 3_1}$	AA-permease	ApcT/3gia [n] AdiC/311 ^a [n] AdiC/3ncy [n]	<i>Methanocaldococcus</i> <i>E. coli</i> <i>Salmonella</i>
$S_{3_1 4_1 3_1}$	SSF	vSGLT/3dh4 [n]	<i>Vibrio parahaemolyticus</i>
$S_{3_1 4_1 3_1}$	BCCT	BetP/2wit ^a [n] PmCaiT/2wsw [n] EcCaiT/2wsx [n]	<i>Brevibacterium</i> <i>Proteus</i> <i>E. coli</i>
$K_{4_1 3_1}$	KARI	KARI/1yve KARI/1yrl KARI/3fr8 [n]	Spinach <i>E. coli</i> Rice
$K_{4_1 4_1}$	PHY	bphP/3c2w cph1/2vea	<i>Pseudomonas</i> <i>Synechocystis</i>
$K_{4_1 4_1}$	PHY	bphP/1ztu bhyB2/2ool	<i>Deinococcus</i> <i>R. palustris</i>
$S_{3_1 3_1 3_1 3_1}$	Cloacin	ColE7/2axc ^a [n] protein B/1rh1 ^a [n]	<i>E. coli</i> <i>E. coli</i>
$S_{3_1 3_1 3_1 3_1}$	S-pyocin	ColE3/1jch [n]	<i>E. coli</i>

Simple motifs are shown in the *SI Appendix* (see *SI Appendix, Tables S1 and S2*), respectively, for knotted and slipknotted proteins. The letters K and S followed by knot type notations indicate whether the entire polypeptide chain of a given protein forms a knot (K) or a slipknot (S), respectively, and the knot types formed by the subchains of a given protein. The pictograms show specific knotting patterns observed for the respective protein families (Pfam classification, ref. 35) as illustrated in Figs. 2–5. Respective protein names, their PDB code, and host species are indicated. An [n] indicates proteins whose knotted pattern are established in this study.

protein in positions that indicate the corresponding protein subchains in the matrix presented in Fig. 2A. The first of these drawings shows that as the C terminus of DehI is clipped progressively, one reaches a point where the remaining C-terminal part no longer pierces the internal loop (indicated by pink in Fig. 2B). Closures of such fragments result in the formation of 4_1 knots. Further clipping of the C terminus results in fragments that no longer pierce the second internal loop (indicated by black in Fig. 2B). The resulting protein fragment forms an unknot but this fragment in fact is a trefoil slipknot, which can be converted to a real trefoil knot by some clipping of its N terminus (see the 3_1 knot in Fig. 2B). The uppermost left drawing presents a protein fragment that, as a result of further C-terminal clipping, is no longer a slipknot because it does not contain any subchains forming nontrivial knots.

The subchains presented to the right of the entire DehI chain illustrate the knotting consequences of progressively clipping the N terminus. We can see that, as the N terminus gets shorter, it retracts first through an imaginary surface spanning the internal loop (indicated by black in Fig. 2B). The placement of the “current” N terminus on that side of the internal loop causes these subchains to form unknots. Interestingly, a further shortening of N termini brings the current N terminus on the original side of the imaginary surface spanning the same internal loop and re-establishes the original knotting of the Stevedore’s knot. This transformation demonstrates that the subchain was in fact a slipknot containing the Stevedore’s knot. The observed direct passages from the Stevedore’s knot to the unknot and then back to the Stevedore’s knot again, upon further shortening of the protein chain, are consistent with the fact that the Stevedore’s knot has unknotting number equal to one (36, 38). Therefore, a slight shortening of the chain can be sufficient to change the resulting

knotting, for example from the Stevedore’s knot to the unknot and vice versa. Further clipping of the N terminus converts the resulting fragment to an unknot that contains a trefoil slipknot, which is revealed as a 3_1 knot upon clipping of its C terminus. This conversion is reflected by moving up in the matrix presented in Fig. 2. Continued clipping of N terminus chains, while maintaining the original C terminus, causes the resulting geometries of these chains to become too simple to form nontrivial knots.

Fig. 2A shows that by removing (or adding) one amino acid residue to the protein fragment, the resulting fragment changes from the Stevedore’s knot to the 4_1 knot, from the Stevedore’s knot to the unknot, from the 4_1 knot to the unknot, and from the 3_1 knot to the unknot. Interestingly, these four pairs of knots are strand passage distance one from each other (38–40), which means that, by a single intersegmental strand passage, it is possible to pass from one knot to the other. In fact, as a given protein subchain with a complex geometry is progressively clipped, one can select a perspective from which one can observe a switch from the majority of closures occurring “above” some part of the chain to the majority of closures occurring “below” that part of the chain. This phenomena is conceptually analogous to one intersegmental passage. In the protein configurations analyzed here, we have observed that neighboring knot territories, marked with different colors in the matrices presented in Fig. 2, are formed by pairs of knots that are strand passage distance one from each other. In Fig. 2, we also see that to pass from 6_1 to 3_1 or from the 4_1 knot to 3_1 one needs to pass through the territory of a different knot type (the unknot in this case). Again, this is consistent with the strand passage distance being two between these two pairs of knots (38–40).

The pattern formed by matrix entries identifying knot types formed by all subchains of an analyzed protein, such as this

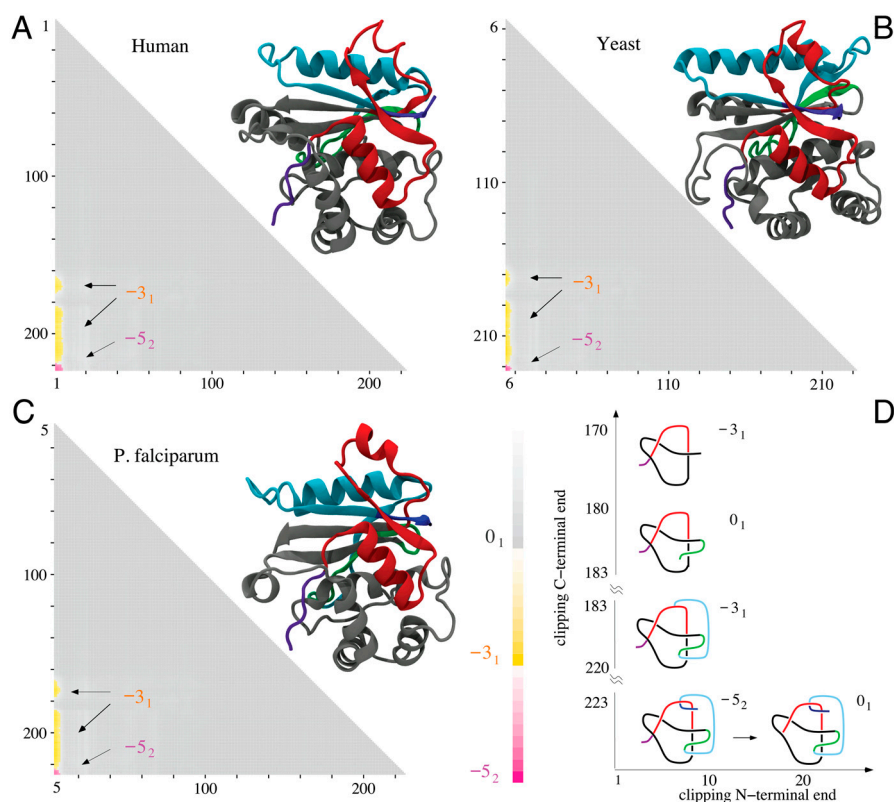


Fig. 3. Molecular structures and matrix presentation for ubiquitin C-terminal hydrolases from (A) human, (B) yeast, and (C) *P. falciparum* plasmodium cells form the same knotting motif, $K5_2 3_1 3_1$. Notice that in all three cases the proteins form 5_2 knots with nearly the same sizes and positions with respect to a linear map of their polypeptide chains. In all cases, the 5_2 knot is unknotted by removing a few amino acids from the N terminus, whereas removing a similar number of amino acids from its C terminus transforms the remaining portion of the protein into a 3_1 knot. (D) Schematic drawings reflecting the overall structure of ubiquitin C-terminal hydrolases explain how the 5_2 knot is converted into an unknot or 3_1 knot depending which end is trimmed.

formed in Fig. 2A, constitutes a very complete characterization of protein knotting. Therefore, we propose to call such patterns “knotting fingerprints” of proteins. The biological significance of the complex knotting of the DehI protein is not yet known. Other proteins with similar catalytic activity have not yet been crystallized and therefore, it is not known whether this complex knotting is evolutionarily conserved.

The 5₂ Protein Knot The second most complex knot observed in proteins is the knot 5₂. This knot was originally detected in two functionally related proteins but originating from human and yeast cells (4). Both proteins belong to ubiquitin C-terminal hydrolases, and their function is to rescue ubiquitin, a small protein that marks and directs other proteins for destruction within supramolecular protein complexes known as proteasomes. The ubiquitin marking is a physiological process by which the concentration of various proteins in eukaryotic cells is regulated not only on the level of their synthesis but also on the level of their degradation. The ubiquitin tag directs a protein to be passed into the narrow channel of the proteasome, where it is then digested into short polypeptides. It would be very costly for cells to digest ubiquitin with each protein marked for destruction, which is why ubiquitin is removed from proteins destined for degradation just before they enter proteasomes. This removal is performed by ubiquitin C-terminal hydrolase. It has been proposed that the knotted structure of ubiquitin C-terminal hydrolase protects this enzyme from accidental entrance into the narrow channel of proteasomes (4). Fig. 3 shows the results of our knotting analysis of ubiquitin C-terminal hydrolases isolated from (i) human, (ii) yeast, and (iii) plasmodium cells. We can see that all three proteins not only form the same knot type but also their knotting fingerprints are very similar. In each case, it suffices to clip off several amino acids from the N terminus to completely unknot the protein. Clipping from C terminus is more interesting because, after clipping just a few amino acids, the remaining subchains form 3₁ knots. A further clipping produces first a slipknot and then again a 3₁ knot, which after further clipping turns to an unknot. Fig. 3D, showing essential geometric features of all three ubiquitin C-terminal hydrolases, illustrates how a progressive clipping of the polypeptide chain forming the 5₂ knot can lead to the formation of a 3₁ knot when one end is clipped and to the creation of an unknot when the other end is clipped.

The direct passage from 5₂ to the unknot is consistent with the fact that the 5₂ knot has unknotting number equal to one. The nearly perfect conservation of knotting fingerprints in ubiquitin C-terminal hydrolases from such evolutionary distant organisms as yeast, plasmodium, and human is even more remarkable if one considers that human and yeast proteins have 32% of sequence identity (41, 42), yeast and plasmodium 28%, and plasmodium and human (UCHL5) 25% (all combinations are shown Table 2).

Coupled Figure-Eight Trefoil Slipknot Motif. An interesting knotting motif consisting of coupled figure-eight trefoil slipknots was originally observed by King et al. (2) in the case of the transmembrane protein LeuT(Aa), a bacterial homolog of neurotransmitter transporters. Our knotting analysis of the PDB entries reveals

Table 2. Sequence identity between proteins with K5₂3₁3₁

Name/name	Source/source	PDB/PDB	ID%
UCHL3/UCHL1	human/human	1xd3/3irt	55
UCHL3/UCHL3	human/Plasmodium	1xd3/2wdt	37
UCHL3/UCHL5	human/human	1xd3/3a7s	30
UCHL3/Yuh1	human/yeast	1xd3/1cmx	32
UCHL3/UCHL1	Plasmodium/human	2wdt/3irt	34
UCHL3/UCHL5	Plasmodium/human	2wdt/3a7s	25
UCHL3/Yuh1	Plasmodium/yeast	2wdt/1cmz	28
UCHL5/Yuh1	human/yeast	3a7s/1cmz	25

that many transmembrane proteins with transporter functions have this knotting motif (see Table 3).

Fig. 4A and B present our knotting analysis of the LeuTAA and BetP proteins. The matrix presentations show that the entire proteins are slipknots (i.e., the entire chains form unknots), but contain distinct subchains that form 4₁ and 3₁ knots. Fig. 4C shows the essential geometric features of these proteins. This figure shows how the truncation of the N terminus creates subchains forming 3₁ knots and how the truncation of the C terminus creates fragments forming 4₁ knots. Interestingly, one must clip both ends of the fragment forming the 4₁ knot to convert it to a fragment that forms the 3₁ knot. The schematic drawings in Fig. 4C also explain why extending the C-terminal portion of the protein forming the 3₁ fragment leads first to slipknotted fragments and only later reestablishes the 3₁ knot. Fig. 4A and B show that, to pass from the 4₁ knot territory to a 3₁ knot territory, one must pass through an unknot territory. This behavior is consistent with the fact that the 3₁ and 4₁ knots are strand passage distance two from each other.

Our analysis of the PDB entries reveals that this complex knotting is conserved across different families of transmembrane proteins and across widely divergent microbes (see Table 3). All of these proteins are membrane cotransport proteins. They share a five-helix inverted repeat motif, which has recently emerged as one of the largest structural classes of secondary active transporters. The similarity between these proteins is shown in Table 3, whereas explanations of abbreviated names of corresponding protein families are listed in the *SI Appendix*. All of these newly characterized slipknot-forming proteins share less than 23% similarity and less than 12% identity to other members of the SNF family. The lowest sequence identity, 6%, is observed between

Table 3. Sequence identity between proteins with the S3₁4₁3₁ motif

Name/name	Source/source	PDB/PDB	ID%
SNF/NCS1	<i>Aquifex/M. liquefaciens</i>	2a65/2jlo	11
SNF/AA	<i>-Methanocaldococcus</i>	-/3gia	9
SNF/-	<i>-E. coli</i>	-/3111	12
SNF/-	<i>-Salmonella</i>	-/3ncy	11
SNF/SSF	<i>-Vibrio</i>	-/3dh4	9
SNF/BCCT	<i>-Corynebacterium</i>	-/2wit	12
SNF/BCCT	<i>-Proteus mirabilis</i>	-/2wsw	11
SNF/BCCT	<i>-E. coli</i>	-/2wsx	11
NCS1/AA	<i>M. liquefaciens/Methanocaldococcus</i>	2jlo/3gia	9
NCS1/-	<i>-E. coli</i>	-/3111	11
NCS1/-	<i>-Salmonella</i>	-/3ncy	12
NCS1/SSF	<i>-Vibrio parahaemolyticus</i>	-/3dh4	12
NCS1/BCCT	<i>-Corynebacterium</i>	-/2wit	8
NCS1/BCCT	<i>-Proteus mirabilis</i>	-/2wsw	9
NCS1/BCCT	<i>-E. coli</i>	-/2wsx	10
SSF/AA	<i>Vibrio/Methanocaldococcus</i>	3dh4/3gia	11
SSF/-	<i>-E. coli</i>	-/3111	9
SSF/-	<i>-Salmonella</i>	-/3ncy	6
SSF/BCCT	<i>-Corynebacterium</i>	-/2wit	11
SSF/BCCT	<i>-Proteus mirabilis</i>	-/2wsw	10
SSF/BCCT	<i>-E. coli</i>	-/2wsx	12
BCCT/AA	<i>Corynebacterium/Methanocaldococcus</i>	2wit/3gia	11
BCCT/-	<i>Proteus mirabilis/-</i>	2wsw/-	9
BCCT/-	<i>E. coli/-</i>	2wsx/-	9
BCCT/AA	<i>Corynebacterium/E. coli</i>	2wit/3111	9
BCCT/-	<i>Proteus mirabilis/-</i>	2wsw/-	11
BCCT/-	<i>E. coli/-</i>	2wsx/-	9
BCCT/AA	<i>Corynebacterium/Salmonella</i>	2wit/3ncy	8
BCCT/-	<i>Proteus mirabilis/-</i>	2wsw/-	10
BCCT/-	<i>E. coli/-</i>	2wsx/-	8
BCCT/BCCT	<i>Proteus mirabilis/E. coli</i>	2wsw/2wsx	89
BCCT/BCCT	<i>Proteus mirabilis/Corynebacterium</i>	2wsw/2wit	25
AA/AA	<i>Methanocaldococcus/E. coli</i>	3gia/3111	18
AA/AA	<i>Methanocaldococcus/Salmonella</i>	3gia/3ncy	16
AA/AA	<i>E. coli/Salmonella</i>	3111/3ncy	82

Table 4. Sequence identity between proteins with zigzag motif, $S_{3_1 3_1 3_1}$

Name/name	PDB/PDB	ID%
ColE7/ColE7	2axc/2bau	62
ColE7/protein B	2axc/1rh1	24
ColE7/ColE3	2axc/1jch	29
Protein B/ColE7	1rh1/2bau	20
Protein B/ColE3	1rh1/1jch	10
ColE3/ColE7	1jch/2bau	68

Knotted Fingerprint of Proteins with Simple Knot Types

There is a relatively large group of proteins that can be classified as 3_1 knots or which show the presence of a single 3_1 slipknot region in their backbones. The knotting notation of these proteins would then be simply K_{3_1} or S_{3_1} , respectively. When one looks closely at their knotting fingerprints, we see that these proteins separate into clearly distinct groups (see *SI Appendix, Tables S1 and S2*). As might be expected, knotted proteins belonging to the same family show similar knotting fingerprints, whereas proteins belonging to different families vary greatly in their knotting fingerprints despite the fact that they have the same overall knotting notation. The strong conservation of the knotting fingerprint, despite significant sequence variance within the individual families of proteins containing simple knots and slipknots, indicates that these relatively simple knotting motifs carry an important functional advantage that has been maintained during their evolution.

The Borders of Knotted Domains Coincide with the Position of Conserved Hinge Sites, Which Are Important for Folding of Knotted Proteins

To understand how knotting fingerprints can be conserved in related knotted proteins with largely diverging sequences, we investigated the location of conserved amino acids in these proteins. We are interested especially in understanding which structural elements correspond to the regions of the knotting fingerprints where a small change in the length of the analyzed subchain leads to the formation of unknots, whereas a further length change leads to the formation of the original knot type or of another knot type. In Fig. 6, these regions of the knotting fingerprints and the corresponding portions of polypeptide chain are marked with dashed lines.

First, we analyzed the location of strictly conserved amino acids in five proteins from the family of ubiquitin C-terminal hydrolases, all of which have the same knotting notation $K_{5_2 3_1 3_1}$ (see Table 1). Three of these proteins are of human origin, one is from yeast, and one is from *Plasmodium falciparum* (see Table 1). Fig. 6A shows the location of all 19 strictly conserved amino acids in these five proteins (the alignment was done using the program Muscle with manual adjustments; ref. 43) and how their position relates to the knotting fingerprint of yeast ubiquitin C-terminal hydrolase. One 15 amino acid long protein region (marked by two dashed lines in Fig. 6A) is highly conserved as it groups six strictly conserved amino acids. This amino acid grouping is the region in which changing the length of the analyzed polypeptide chain leads to a passage from a 3_1 knot to an unknot and again to a 3_1 knot. Among these six conserved amino acids are three glycines, which are known to preferentially locate in protein hinge sites (44). Indeed, an inspection of secondary structure plots of C-terminal hydrolases (<http://www.rcsb.org/pdb/explore/remediatedSequence.do?structureId=1cmx>) reveals that these three glycines are located in protein regions with high potential flexibility.

Subsequently, we analyzed the sequence conservation within the proteins with the next most complex knotting notation—i.e., $S_{3_1 4_1 3_1}$ (see Table 1). Because very similar knotting fingerprints were observed within five protein families (SNF, NCS1, AA-permease, SSF, and BCCT), we compared protein sequences of all nine proteins from these families for which the structure is known. Because the sequence conservation of proteins from different families is generally low, we consider as “highly conserved” those amino acids that were present at least six times in a given position within the aligned sequences of the nine proteins. Fig. 6B shows the location of all the amino acids that fulfilled these criteria. In the case of proteins with the knotting notation $S_{3_1 4_1 3_1}$ there are three protein regions where changing the length of the analyzed subchains leads to unknotting, whereas a further length change produces a knotted state (these regions are marked by dashed lines on Fig. 6B). Whereas the entire N-terminal portion is necessary to form a 4_1 slipknot, trimming about 25 amino acids from the N-terminus precludes the formation of any knotted structures. A further trimming allows the formation of 3_1 knots. Interestingly, in the narrow interval transitioning from the 4_1 knot to the unknot and then to the 3_1 knot, we observe one of the highly conserved glycines. In the C-terminal halves of these

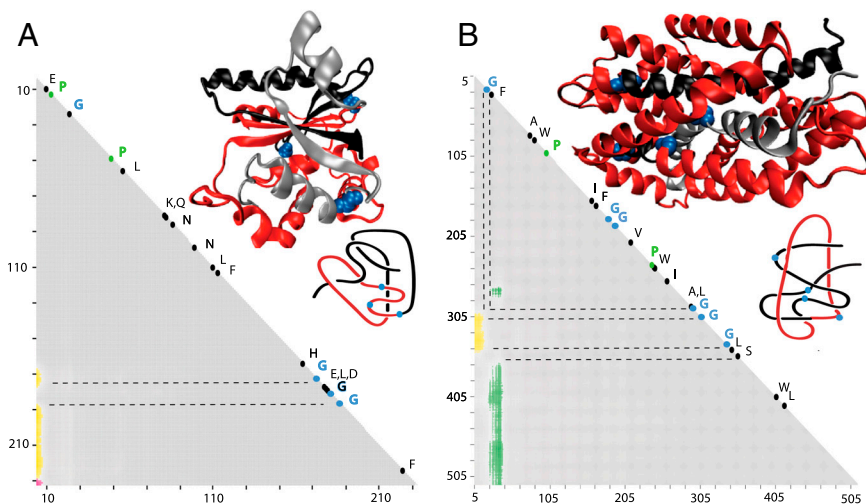


Fig. 6. Sequence conservation in related proteins with complex knotting fingerprints. (A) Ubiquitin C-terminal hydrolase (knot notation $K_{5_2 3_1 3_1}$). (B) Five families of proteins with knotting notation $S_{3_1 4_1 3_1}$ (see Table 1). The positions of the protein regions where varying the length of the analyzed subchain leads to a passage from a knot to the unknot and then again to a knot are indicated with dashed lines. These regions show strong sequence conservation with a high proportion of conserved glycines. The placement of these glycines can be seen in the molecular structures of representative proteins belonging to the analyzed groups (Yuh1 and LeuT for A and B, respectively) and also on the schematic drawings.

proteins there are two approximately 20 amino acid long regions where changes in the analyzed subchain length result in a change from the 3_1 knot to the unknot and then to the 4_1 knot (or vice versa). In one of these regions, we observe two highly conserved glycines, whereas the second region contained one highly conserved glycine. An inspection of the secondary structure plots (<http://www.rcsb.org/pdb/explore/remediatedSequence.do?structureId=2A65>) reveal that at least three out of four of the highly conserved glycines can be involved in hinge formation.

For other proteins with complex knotting signatures, the number of related proteins that have been crystallized is too small for a meaningful analysis of sequence conservation. Our analysis of sequence conservation in proteins with very similar knotting fingerprints reveals that glycines were most frequently represented among conserved amino acids (10 out of 31, see Fig. 6). This very high proportion of conserved glycines may seem surprising because the majority of conserved glycines are located in regions that are likely to serve as hinge sites, which in general are known to have a low sequence conservation (44). However, as the folding of proteins forming knots and slipknots is more complex than that of proteins with trivial knotting, it is likely that hinges involved in their folding may need special properties that require much stricter sequence conservation. In fact, an earlier study that used coarse grained molecular modeling to follow the folding of knotted proteins showed that sharp turns involving glycines and prolines are instrumental in correctly folding knotted proteins (5).

Discussion

Our comprehensive analysis of proteins with complex knotting shows that not only is the overall knot type formed by these proteins conserved but also the precise relative positions of the protein segments forming the knot, which as such determine knotting fingerprints of the knotted proteins. This knotting conservation persists despite significant sequence divergence within the respective protein families. Interestingly, the strongest sequence conservation is observed in protein regions that are likely to serve as hinges during the folding of knotted proteins. Protein hinges or flexible joints regions are generally known to show very poor sequence conservation among proteins belonging to the same family but we observed an opposite trend for related knotted proteins. The instrumental role of hinges or flexible joints in the folding of knotted proteins was noted in earlier studies (27). Our observation of high sequence conservation within hinges in knotted proteins indicates that these hinges have some special properties that are crucial for efficient folding. Further studies will be needed to elucidate the role of these conserved hinges in the process of folding knotted proteins.

We have discovered two previously unknown families of knotted proteins and five families of proteins with slipknots (see Table 1 and *SI Appendix, Tables S1 and S2*). To our knowledge, this brings the number of distinct protein families where the native backbone can be thought of as forming a knot to 18, and the number of distinct protein folds with slipknots to 17. In the five families of proteins that form transmembrane transporting

channels, the slipknot loops seem to strap together several of transmembrane α -helices. This architecture may stabilize the channels during their transporter and symporter action. It is known that, for entropic reasons, knots in random walks have the tendency to form tight-knotted domains (31, 45). It is therefore possible that some pathways of protein knotting may preferentially form tight protein knots. Furthermore, territories of distinct knot types in direct contact in the matrix representations were knot types that were strand passage distance one from each other, something that had not been recognized to date. Because descriptors such as knot types are more global than the geometrical descriptors used to determine fold types, our analysis reveals an additional level of functional significance in protein structures.

Materials and Methods

The PDB dataset (28), as of April 16, 2011, contained 74,223 entries. From the resulting dataset, we retained all proteins with chain length more than 45 aa. In addition to previous studies (4, 25), we accepted chains with more than 1,000 aa and sequences with some missing C^α coordinates. In the case of protein structures with unresolved parts, we "inserted" the missing portions by modeling the structure or by adding a straight line connection. In the modeling procedure, the proteins missing segments shorter than 10 aa were reconstructed based on ref. 46. However, cases such as UCHL1, when 23 C^α atoms were unresolved, were modeled based on sequence similarity or geometrical similarity using software (47). In cases where the missing portions could be connected unambiguously by a straight line (without introducing a steric clash with the rest of structures), we simply added such a line segment. This procedure resulted in a total of 42,389 protein chains. The longest chain in our dataset has 1,223 aa.

As a first step in identifying knots and slipknots in the dataset of 42,389 proteins, we applied the Koniaris–Muthukumar–Taylor algorithm (34). This dataset was further evaluated, as described below, in order to detect only correctly knotted and slipknotted proteins. We computed the knot distribution for each subchain of each protein as follows: For each protein subchain, we create 100 closed knots by connecting the endpoints of the subchain to 100 points on a large sphere. This sphere is centered at the center of mass of the entire protein's C^α atoms and the radius is 100 times the greatest distance from the center of mass to any C^α atom. Although previous papers had used random points on the sphere, individual samples from random distributions are rarely uniform. Thus, we used software (<http://members.ozemail.com.au/~llan/mpol.html>) to generate a (nearly) uniform set of 100 points on a unit sphere, and then rescaled them to be points on the large sphere.

For each of the 100 closed knots formed per subchain, we computed the HOMFLYPT polynomial (48, 49) using the Ewing–Millett program (50) to determine the knot type. Although the HOMFLYPT polynomial cannot separate all knot types (i.e., there are different knot types with the same HOMFLYPT polynomial), the knot types found in proteins (to date) have been quite simple, so the HOMFLYPT polynomial does not misclassify knot types. We then compute the percentage of the closures forming each knot type and classify the knot type of the subchain, indicated by the color of the square, to be the knot type with the highest percentage.

ACKNOWLEDGMENTS. J.I.S. and J.N.O. were supported by the Center for Theoretical Biological Physics, sponsored by the National Science Foundation (NSF) (Grant PHY-0822283), and by NSF-MCB-1051438. A.S. was supported by the Swiss National Science Foundation (Grant 31003A-116275). E.J.R. was supported by NSF Grants 0810415 and 1115722.

- Mansfield ML (1994) Are there knots in proteins? *Nat Struct Biol* 1:213–214.
- King NP, Yeates EO, Yeates TO (2007) Identification of rare slipknots in proteins and their implications for stability and folding. *J Mol Biol* 373:153–166.
- Lua RC, Grosberg AY (2006) Statistics of knots, geometry of conformations, and evolution of proteins. *PLoS Comput Biol* 2:e45.
- Virnau P, Mirny LA, Kardar M (2006) Intricate knots in proteins: Function and evolution. *PLoS Comput Biol* 2:e122.
- Sulkowska JI, Sulkowski P, Onuchic JN (2009) Dodging the crisis of folding proteins with knots. *Proc Natl Acad Sci USA* 106:3119–3124.
- King NP, Jacobitz AW, Sawaya MR, Goldschmidt L, Yeates TO (2010) Structure and folding of a designed knotted protein. *Proc Natl Acad Sci USA* 107:20732–20737.
- Sulkowska JI, Sulkowski P, Szymczak P, Cieplak M (2008) Stabilizing effect of knots on proteins. *Proc Natl Acad Sci USA* 105:19714–19719.
- Mallam AL, Rogers JM, Jackson SE (2010) Experimental detection of knotted conformations in denatured proteins. *Proc Natl Acad Sci USA* 107:8189–8194.
- Prentiss MC, Wales DJ, Wolynes PG (2010) The energy landscape, folding pathways and the kinetics of a knotted protein. *PLoS Comput Biol* 6:e1000835.
- Noel JK, Sulkowska JI, Onuchic JN (2010) Slipknotting upon native-like loop formation in a trefoil knot protein. *Proc Natl Acad Sci USA* 107:15403–15408.
- Shakhnovich E (2011) Protein folding: To knot or not to knot? *Nat Mater* 10:84–86.
- Sayre TC, Lee TM, King NP, Yeates TO (2011) Protein stabilization in a highly knotted protein polymer. *Protein Eng Des Sel* 24:627–630.
- Alam MT, et al. (2002) The importance of being knotted: Effects of the C-terminal knot structure on enzymatic and mechanical properties of bovine carbonic anhydrase II. *FEBS Lett* 519:35–40.
- Wang T, Arakawa H, Ikai A (2001) Force measurement and inhibitor binding assay of monomer and engineered dimer of bovine carbonic anhydrase B. *Biochem Biophys Res Commun* 285:9–14.
- Mallam AL, Jackson SE (2007) A comparison of the folding of two knotted proteins: YbeA and YibK. *J Mol Biol* 366:650–665.

16. Bornschlogl T, et al. (2009) Tightening the knot in phytochrome by single-molecule atomic force microscopy. *Biophys J* 96:1508–1504.
17. Ohta S, et al. (2004) Origin of mechanical strength of bovine carbonic anhydrase studied by molecular dynamics simulation. *Biophys J* 87:4007–4020.
18. Tkaczuk KL, et al. (2007) Structural and evolutionary bioinformatics of the SPOUT superfamily of methyltransferases. *BMC Bioinformatics* 8:73.
19. Lai YL, Yen SC, Yu SH, Hwang JK (2007) pKNOT: The protein KNOT web server. *Nucleic Acids Res* 35:W420–W424.
20. Wallin S, Zeldovich KB, Shakhnovich EI (2007) The folding mechanics of a knotted protein. *J Mol Biol* 368:884–893.
21. Dzubielia J (2009) Sequence-specific size, structure, and stability of tight protein knots. *Biophys J* 96:831–839.
22. Huang L, Makarov DE (2008) Translocation of a knotted polypeptide through a pore. *J Chem Phys* 129:121107.
23. Faisca PFN, et al. (2010) The folding of knotted proteins: Insights from lattice simulations. *Phys Biol* 7:016009.
24. Tuszynska I, Bujnicki JM (2010) Predicting atomic details of the unfolding pathway for YibK, a knotted protein from the SPOUT superfamily. *J Biomol Struct Dyn* 27:511–520.
25. Potestio R, Micheletti C, Orland H (2010) Knotted versus unknotted proteins: evidence of knot-promoting loops. *PLoS Comput Biol* 6:e1000864.
26. Andreeva A, Murzin AG (2010) Structural classification of proteins and structural genomics: New insights into protein folding and evolution. *Acta Crystallogr Sect F Struct Biol Cryst Commun* 66:1190–1197.
27. Bölinger D, et al. (2010) A Stevedore's protein knot. *PLoS Comput Biol* 6:e1000731.
28. Berman HM, et al. (2000) The protein data bank. *Nucleic Acids Res* 28:235–242.
29. Taylor WR (2000) A deeply knotted protein structure and how it might fold. *Nature* 406:916–919.
30. Millett K, Dobay A, Stasiak A (2005) Linear random knots and their scaling behavior. *Macromolecules* 38:601–606.
31. Katritch V, Olson WK, Vologodskii A, Dubochet J, Stasiak A (2000) Tightness of random knotting. *Phys Rev E Stat Nonlin Soft Matter Phys* 61:5545–5549.
32. Marcone B, Orlandini E, Stella AL, Zonta F (2005) What is the length of a knot in a polymer? *J Phys A Math Gen* 38:L15–L21.
33. Tubiana L, Orlandini E, Micheletti C (2011) Probing the entanglement and locating knots in ring polymers: A comparative study of different arc closure schemes. *Prog Theor Phys Suppl* 191:192–204.
34. Koniaris K, Muthukumar M (1991) Self-entanglement in ring polymers. *J Chem Phys* 95:2873–2881.
35. Finn RD, et al. (2006) Pfam: Clans, web tools and services. *Nucleic Acids Res* 34:D247–D251.
36. Taylor WR (2005) Protein folds, knots and tangles. *Physical and numerical models in knot theory*, eds JA Calvo, KC Millet, EJ Rawdon, and A Stasiak (World Scientific, Singapore), pp 171–202.
37. Schmidberger JW, Wilce JA, Weightman AJ, Whisstock JC, Wilce MCJ (2008) The crystal structure of Dehl reveals a new alpha-haloacid dehalogenase fold and active-site mechanism. *J Mol Biol* 378:284–294.
38. Darcy IK, Summers DW (2000) Rational tangle distance on knots and links. *Math Proc Cambridge Philos Soc* 128:497–510.
39. Flammini A, Maritan A, Stasiak A (2004) Simulations of action of DNA topoisomerases to investigate boundaries and shapes of spaces of knots. *Biophys J* 87:2968–2975.
40. Darcy IK, Scharein RG, Stasiak A (2008) 3D visualization software to analyze topological outcomes of topoisomerase reactions. *Nucleic Acids Res* 36:3515–3521.
41. Hasegawa H, Holm L (2009) Advances and pitfalls of protein structural alignment. *Curr Opin Struct Biol* 19:341–348.
42. Holm L, Sander C (1996) Mapping the protein universe. *Science* 273:595–602.
43. Edgar RC (2004) MUSCLE: Multiple sequence alignment with high accuracy and high throughput. *Nucleic Acids Res* 32:1792–1797.
44. Flores SC, Lu LJ, Yang J, Carriero N, Gerstein MB (2007) Hinge atlas: Relating protein sequence to sites of structural flexibility. *BMC Bioinformatics* 8:167.
45. Orlandini E, Stella AL, Vanderzande C (2009) The size of knots in polymers. *Phys Biol* 6:025012.
46. Fernandez-Fuentes N, Zhai J, Fiser A (2006) ArchPRED: A template based loop structure prediction server. *Nucleic Acids Res* 34:W173–W176.
47. Grant BJ, Rodrigues AP, ElSawy KM, McCammon JA, Caves LS (2006) Bio3D: An R package for the comparative analysis of protein structures. *Bioinformatics* 22:2695–2696.
48. Freyd P, et al. (1985) A new polynomial invariant of knots and links. *Bull Am Math Soc* 12:239–246.
49. Przytycki JH, Traczyk P (1987) Invariants of links of Conway type. *Kobe J Math* 4:115–139.
50. Ewing B, Millett KC (1997) Computational algorithms and the complexity of link polynomials. *Progress in Knot Theory and Related Topics* (Hermann, Paris), pp 51–68.

Supplementary Material

Conservation of complex knotting and slipknotting patterns in proteins

J. I. Sulkowska, E. J. Rawdon, K. C. Millett, J.N. Onuchic and A. Stasiak

Guide to the abbreviated names of protein families listed in Table 1 (in the main text) and in tables S1 and S2.

AA-permease - amino acid permeases, ART - arginine ADP-ribosyltransferase family, BCCT - betaine/carnitine/choline transporters, DUF - domains of unknown function, EMG1 - EMG1/NEP1 methyltransferases, Herpes_TK - herpes virus thymidine kinase, MetaL - Metalloenzymes, NCS1 - nucleobase-cation-symport-1 transporters, NPP- Nucleotide pyrophosphatases, PHY - Phytochrome region family, PmbA-TldD - Putative modulators of DNA gyrase, Pyr_Redox_2 - Pyridine nucleotide-disulphide oxidoreductases, RbsD/FucU Ribose/fucose transport protein family, SAM synthetase - S-adenosylmethionine synthetases, SDF - sodium:dicarboxylate symporters, SNF - Sodium: neurotransmitter symporters, SpoU_methylase - SpoU rRNA Methylase family, SPOUT-MTase - Predicted SPOUT methyltransferase protein family, SSF - sodium:solute symporters, Trm 56 - tRNA ribose 2'-O-methyltransferases, tRNA_m1G_MT - tRNA (Guanine-1)-methyltransferases, virC2 - virulence C2 protein family.

Explanation of notation used in Tables S1 and S2. In several cases, the structure determination of the proteins was not complete, resulting in an uncertainty concerning the position of some fragments. For the knotting analysis, we replaced missing fragments with a straight line if the missing peptide could be placed in the vicinity of the straight line without clashing with the rest of the chain (these cases are indicated with *a*). With *b* we indicated the cases, where the missing peptide had to follow an arc to avoid a steric clash with the rest of the determined protein structure An [n] indicates proteins whose knotted pattern are established in this study.

Table S1: Simple knotting patterns (S_3 and S_3) in slipknotted proteins. The pictograms show specific knotting patterns observed for the respective protein families (Pfam classification, [1]). Respective protein names, their PDB code and host species are indicated. Dark green and light green colors indicate right- and left-handed 3_1 knot, respectively.

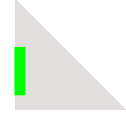
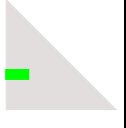
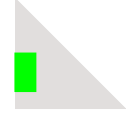
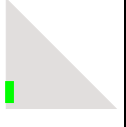
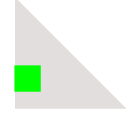
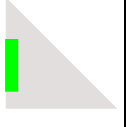

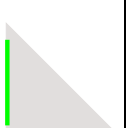
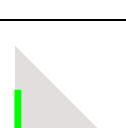


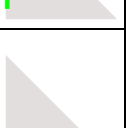
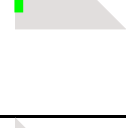
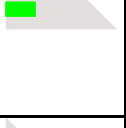
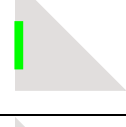
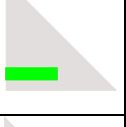
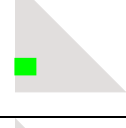
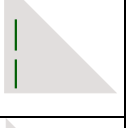
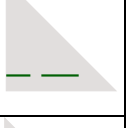

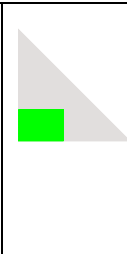

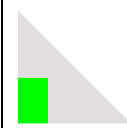
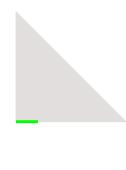
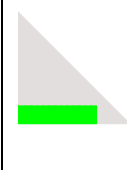
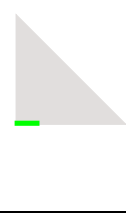
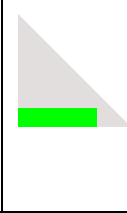
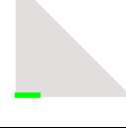
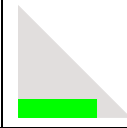

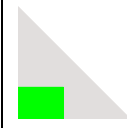

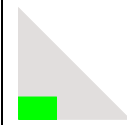
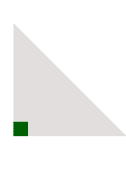
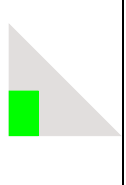

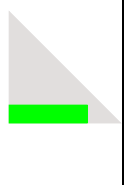
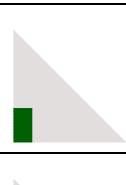
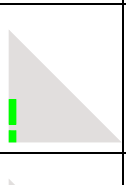
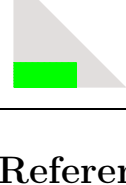
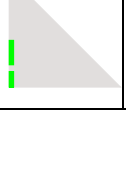
Motif	Family	Protein/PDB	Source	Motif	Family	Protein/PDB	Source
	Alk phosphatase	AP/2x98 [n]	Halobacteriu		Alk sulfatase	PUF/3lxq	Vibrio
	Alk phosphatase	AP/1ew2 AP/1shn	Human Shrimp		DUF	DUF1874/2j85 Protein 114/2x4i ^a [n]	Rudivirus Rudivirus
	Alk phosphatase	AP/1alk	E.coli		NPP	PhnA/1ei6[n] -/2gso[n]	Pseudomonas Xanthomonas
	Alk phosphatase	TAP/2iuc ^a	Antarctic bacterium		Herpes _TK	-/1osn ^a [n] HSV1-T/1p7c EHV4- TK/1p6x	Varicellovirus Simplexvirus Varicellovirus
	Alk phosphatase	SCAP/3a52 [n] -/3e2d [n]	Shewanella Vibrio		MetaL	PMG/1ejj[n] PMG/3igy[n] PMG/2ify[n]	Geobacillus Leishmania Bacillus anthracis
	Alk sulfatase	PALK/2vqr[n] pehA/2w8s[n] YidJ/2qzu[n] YidJ/3b5q[n] Putative arylsulfatase/3ed4	Agrobacterium Burkholderia Bacteroides Bacteroides E.coli		RbsD / FucU	-/2wcu[n] FuCu/3mvk[n] -/3e7n[n] Atu2016/2ob5[n] RbsD/1ogc[n]	Mouse Bifidobacteriu Salmonella Agrobacterium Bacillus subtilis
	Alk sulfatase	AS/1hdh[n]	Pseudomonas		PmbA- TldD	PmbA/3qtd ^a [n] PmbA/1vpb[n] PmbA/1vl4 ^a [n]	Pseudomonas Bacteroides Thermotoga
	Alk sulfatase	LTA/2w8d[n] LTA/2w5q[n]	Bacillus Staphylococcus		ADP- ribo	ART/1gy0[n]	Rat
	Alk sulfatase	ASA/1auk ^a ASB/1fsu ^a [n]	Human Human		Pyr_ redox_2	AIF/1gv4[n]	Mouse
					SDF	GltPh/1xfh	Pyrococcus horikoshii

Table S2: Simple knotting patterns ($K3_1$ and $K3_13_1$) in knotted proteins. The pictograms show specific knotting patterns observed for the respective protein families (Pfam classification, [1]). Respective protein names, their PDB code and host species are indicated. Dark green and light green colors indicate right- and left- hand 3_1 knot, respectively.

Motif	Family	Protein/PDB	Source	Motif	Family	Protein/PDB	Source
	Carbonic anhydrase	CA I/1hcb CA II/1lug CA II/1v9e CA II/1y7w CA III/1z93 CA III/1fj CA IV/2znc CA IV/1znc	Human Human Bovine D. salina Human Rat Human Mouse		SpoU_methylase	tRNAm/1zjr TRNAm/1v2x tRNAm/3e5y putm/3ic6 -/3onp tRNAm/3n4j[n] tRNAm/3l8u[n] TAR/2ha8	Aquifex Thermus Pseudomallei Neisseria Bordetella Yersinia Streptococcus Human
	Carbonic anhydrase	CA V/1keq	Mouse		SpoU_methylase	-/3ilk ^a	Haemophilus
	Carbonic anhydrase	CA VI/3fe4[n] CA VI/1kop	Human N. gonorrhoeae		SpoU_methylase	RNA2o/1ipa -/1gz0 RRNAm/1x7o RNAm/2i6d rRNA/3gyq YibK/1j85	Thermus E.coli Streptomyces Porphyromonas Streptomyces Haemophilus
	Carbonic anhydrase	CA VIII/2w2j[n] CA IX/3iai[n] CA XII/1jd0 CA XIII/3czv[n] CA XIV/1rj6	Human Human Human Human Mouse		Methyltransferase	rmsE/1nxz rmsE/1vhk ^a -/1v6z PUF/3kw2 ^a [n] PUF/2cx8 PUF/1z85 ^b rsmE/2egv	Haemophilus Bacillus Thermus Porphyromonas Thermus Thermotoga Aquifex
	Carbonic anhydrase	PTPRZ /3jxf[n]	Human		EMG1 methyltransferase	NEP1/2v3k ^a [n] NEP1/3o7b[n] NEP1/3bbd	Saccharomyces Archaeoglobus Methanocaldococcus
	Carbonic anhydrase	PTPRZ /3jxh[n] PTPRZ /3jxg[n]	Human Mouse		Trm56	Trm56/2o3a ^a Trm56/2yy8	Archaeoglobus Pyrococcus
	virC2	-/2rh3	Agrobacterium		SPOUT_MTase	YbeA/1ns5 ^a YbeA/1o6d YbeA/1vh0 YbeA/1to0 ^a	E.coli Thermotoga Staphylococcus Bacillus

Motif	Family	Protein/PDB	Source	Motif	Family	Protein/PDB	Source
	Ribbon-helix-helix	PUF/2efv	Methanocaldococcus		tRNA _m1G _MT	TrmD/3ief TrmD/1uaj ^a TrmD/3ky7 ^a TrmD/1p9p ^a TrmD/3knu ^a	Bartonella Haemophilus Staphylococcus E.coli Phagocytophilum
	U2 snRNP	PHF5/2k0a	Saccharomyces		DUF	2168/3dcm[n] 358/2qvv ^a [n] 358/2qmm 358/3aia[n] 171/1k3r	Thermotoga Vibrio cholerae Archaeoglobus Methanocaldococcus Methanothermobacter
	designed protein	-/3mlg	Helicobacter		SAM syn- thetase	-/2obv	Human
	OTCace	AOTCase/1yh1 AOTCase/1js1	Xanthomonas Bacteroides		SAM syn- thetase	-/1fug -/1qm4 ^a -/3rv2 ^a [n] -/3iml ^a	E.coli Rat Mycobacterium pseudomallei group

References

- [1] Finn RD, et al (2006) Pfam: clans, web tools and services. *Nucleic Acids Res.* 34: D247-D251.